

Published in final edited form as:

*Nat Neurosci.* 2010 December ; 13(12): 1519–1525. doi:10.1038/nn.2685.

## Postsynaptic TRPV1 triggers cell-type specific LTD in the nucleus accumbens

Brad A. Grueter, Gabor Brasnjo, and Robert C. Malenka\*

Nancy Pritzker Laboratory, Dept. of Psychiatry and Behavioral Sciences, Stanford University School of Medicine, Palo Alto, CA, 94304

### Abstract

Synaptic modifications in the nucleus accumbens (NAc) play a key role in adaptive and pathological reward-dependent learning. Medium spiny neurons (MSNs), the major cell type in the NAc, participate in two parallel circuits that subserve distinct behavioral functions yet little is known about differences in their electrophysiological and synaptic properties. Here we utilize bacterial artificial chromosome (BAC) transgenic mice to show that synaptic activation of group I metabotropic glutamate receptors (mGluRs) in indirect but not direct pathway NAc MSNs lead to production of endocannabinoids, which in addition to activating presynaptic CB1 receptors to trigger endocannabinoid-mediated long-term depression (eCB-LTD), activated postsynaptic TRPV1 channels that triggered a form of LTD due to endocytosis of AMPA receptors. These results reveal a novel action of TRPV1 channels and demonstrate that the postsynaptic generation of endocannabinoids can modulate synaptic strength in a cell type specific fashion via activation of distinct pre- and postsynaptic targets.

The anatomical connectivity of the NAc positions it as a key interface integrating motivational information from limbic system structures with circuitry controlling motor output in the service of regulating goal-directed behavior<sup>1</sup>. The outputs from the NAc derive from GABAergic MSNs, the activity of which is driven primarily by excitatory inputs from prefrontal cortex, hippocampus and amygdala. These synapses express several forms of plasticity that are thought to be important for a variety of adaptive and pathological forms of behavior including addiction<sup>2, 3</sup>. Specifically, it has been suggested that pathological recruitment or blockade of LTD and long-term potentiation (LTP) in NAc by drugs of abuse may be one of the critical steps in the cascade of neuroadaptations leading to addiction. Furthermore, long-lasting changes in synaptic properties within the NAc are likely to be critical for the maintenance of the addicted state<sup>2-5</sup>.

Over 90% of the cells within the NAc are MSNs, which like MSNs in the dorsal striatum are not homogenous but can be divided into two major subpopulations<sup>1, 6</sup>. Direct pathway MSNs express D1 dopamine (DA) receptors and project directly to midbrain dopamine (DA) centers while indirect pathway MSNs express D2 DA receptors and project to the ventral pallidum, thereby indirectly influencing DA cell activity. Recent studies have demonstrated that direct pathway and indirect pathway MSNs in the dorsal striatum exhibit dramatically different electrophysiological and synaptic properties<sup>6</sup> and that the two subtypes of MSNs play distinct roles in motor behavior and various forms of learning<sup>7, 8</sup>. Surprisingly, however, despite the behavioral importance of plasticity at excitatory synapse

\*Correspondence to: R. Malenka, M.D., Ph.D. Department of Psychiatry and Behavioral Sciences, 1050 Arastradero Rd. Stanford Institutes of Medicine Palo Alto, CA 94304-5485 Tel. 650-724-2730 Fax. 650-724-2753 malenka@stanford.edu.

**Author Contributions** B.A.G., G.B., and R.C.M. designed the experiments, interpreted the results and wrote the paper. B.A.G. and G.B. performed all of the experiments and analyzed the results.

within the NAc in neuropsychiatric disorders such as addiction, very little is known about differences in the cellular and synaptic properties of these two NAc MSN populations.

Utilizing BAC transgenic mice that express EGFP in indirect pathway, D2 DA receptor-expressing MSNs<sup>9</sup>, we have examined the cellular and synaptic properties of these different cell populations in the NAc core using targeted whole-cell patch clamp recording techniques. We found that there are significant differences in the properties of excitatory synapses onto NAc indirect pathway MSNs [D2(+) MSNs] compared to direct pathway synapses and that several of these differences are similar to those previously observed in MSNs in the dorsal striatum. Most importantly, postsynaptic mGluR activation triggered LTD in D2(+) MSNs but not in direct pathway MSNs [D2(-) MSNs]. Surprisingly, however, this cell type specific LTD was reduced but not blocked by a CB1 receptor antagonist indicating that a form of LTD, in addition to eCB-LTD, was present at excitatory synapses on D2(+) MSNs in NAc.

Because lipid signaling molecules, including the endocannabinoid anandamide, can activate TRPV1 (transient receptor potential vanilloid 1) channels<sup>10-13</sup>, which can trigger presynaptic LTD in other brain regions<sup>14, 15</sup>, we performed experiments to test whether TRPV1 channels were required for the CB1 receptor-independent LTD. Our results indicate that mGluR activation in D2(+) MSNs leads not only to eCB-LTD but also to activation of postsynaptic TRPV1 channels that trigger a form of LTD due to endocytosis of AMPARs. In addition, we found that *in vivo* administration of cocaine prevented the generation of both forms of LTD in NAc D2(+) MSNs and that *TRPV1*<sup>-/-</sup> mice exhibit enhanced behavioral sensitization to repeated administration of cocaine. These results reveal a novel, cell type specific form of synaptic plasticity due to activation of postsynaptic TRPV1 channels by an endogenous vanilloid and provide further evidence that TRPV1 channels within the brain have behaviorally significant roles.

## RESULTS

### Electrophysiological and synaptic properties of NAc MSNs

To determine whether, as in the dorsal striatum<sup>6</sup>, the two major subpopulations of MSNs within the NAc core exhibit different electrophysiological and synaptic properties, we prepared slices from BAC transgenic mice, which express EGFP in indirect pathway D2(+) MSNs<sup>9</sup>. Similar to MSNs in the dorsal striatum<sup>6, 16</sup> basal electrophysiological and synaptic properties differed between NAc core indirect pathway, D2(+) and direct pathway, non-D2 expressing [D2(-)] MSNs. Paired-pulse ratios of EPSCs, a measure that inversely correlates with transmitter release probability, were higher in D2(-) MSNs (20 ms  $1.55 \pm 0.10$ ; 50 ms  $1.40 \pm 0.07$ ; 100 ms  $1.21 \pm 0.05$ ; 200 ms  $1.07 \pm 0.04$ , n=15; Fig. 1a) relative to D2(+) MSNs (20 ms  $1.33 \pm 0.07$ ; 50 ms  $1.22 \pm 0.04$ ; 100 ms  $1.12 \pm 0.05$ ; 200 ms  $1.00 \pm 0.04$ , n=18; Fig. 1a). Consistent with these results, the basal frequency of miniature EPSCs (mEPSCs) was greater in D2(+) MSNs than in D2(-) MSNs (Fig. 1b) while the amplitudes of mEPSCs were not different (Fig. 1b).

AMPA-mediated EPSCs (AMPA EPSCs) recorded from both D2(+) and D2(-) MSNs exhibited linear current-voltage relationships and little rectification (Fig. 1c; current ratio at +40 mV versus -80 mV; D2(+)  $0.34 \pm 0.02$ , n = 10; D2(-)  $0.35 \pm 0.02$ , n = 11). However, EPSCs generated in D2(+) cells exhibited a larger ratio of NMDAR EPSCs (measured at +40 mV, 50 ms post-stimulus) to AMPAR EPSCs (peak measured at -80 mV) (Fig. 1d, e; D2(+),  $0.42 \pm 0.04$ , n = 10; D2(-),  $0.28 \pm 0.02$ , n = 11). These results demonstrate that indirect pathway excitatory synapses on D2(+) MSNs in NAc core express several properties that are distinct from those of direct pathway synapses on D2(-) MSNs; they exhibit a higher release probability and a higher proportion of synaptic NMDARs.

Furthermore, NAc core D2(+) MSNs fire a larger number of action potentials in response to fixed current injections than D2(-) MSNs (Fig. 1f, g) indicating that they are intrinsically more excitable.

### Cell type specific LFS LTD in NAc core

We next examined the generation of LTD in indirect pathway and direct pathway MSNs in the NAc core. Although NMDAR-dependent LTD was elicited in both populations of MSNs in response to three bursts of 3 Hz / 5 min afferent stimulation [D2(+),  $77 \pm 6\%$  of baseline,  $n = 5$ ; D2(-),  $81 \pm 7\%$ ,  $n=6$ ; data not shown), a protocol similar to that previously reported to elicit eCB-LTD in NAc MSNs<sup>17</sup> (10 Hz / 5 min: termed LFS) generated robust LTD in D2(+) MSNs but, on average, no LTD in D2(-) MSNs. (Fig. 2a-c: D2(+),  $51 \pm 7\%$  of baseline at 35–40 min post LFS,  $n = 25$ ; D2(-),  $92 \pm 4\%$ ,  $n = 11$ ). The LTD elicited by the LFS protocol in D2(+) MSNs was not affected by the NMDAR antagonist D-APV (100  $\mu$ M) (Fig. 2d:  $47 \pm 10\%$ ,  $n = 6$ ), nor by a D1 DA (SCH23390, 2  $\mu$ M) or a D2 DA receptor antagonist (sulpiride, 10  $\mu$ M) (SCH23390,  $61 \pm 6\%$ ,  $n=4$ ; sulpiride,  $50 \pm 12\%$  of baseline,  $n=6$ ; data not shown). In contrast, the mGluR antagonist LY341495 at a concentration that antagonizes all mGluRs (100  $\mu$ M) prevented LFS LTD in D2(+) MSNs (Fig. 2e:  $95 \pm 5\%$ ,  $n = 6$ ) while a concentration of LY341495 (200 nM) that is specific for group II mGluRs had no effect (Fig. 2e:  $53 \pm 9\%$ ,  $n = 6$ ). The mGluR5 specific antagonist MPEP (10  $\mu$ M) also blocked LFS LTD in the D2(+) MSNs (Fig. 2f:  $93 \pm 5\%$ ,  $n = 5$ ) while the mGluR1 antagonist (LY367385, 100  $\mu$ M) did not ( $36\% \pm 7\%$ ,  $n = 4$ , data not shown).

These results suggest that like eCB-LTD in D2(+) MSNs in the dorsal striatum<sup>16</sup> and that previously reported in the NAc<sup>17</sup>, LFS LTD in NAc core D2(+) MSNs requires activation of the group I mGluR, mGluR5. Consistent with this conclusion, application of the group I mGluR agonist RS-DHPG (100  $\mu$ M) elicited LTD in D2(+) MSNs but not in D2(-) MSNs (Fig. 2g; D2(+),  $66 \pm 4\%$ ,  $n = 14$ ; D2(-)  $103 \pm 7\%$ ,  $n = 5$ ). Following application of DHPG in D2(+) MSNs, LFS LTD was no longer elicited (Fig. 2h:  $99 \pm 20\%$ ,  $n = 4$ ) suggesting that the DHPG-induced LTD occluded the subsequent generation of LFS LTD.

Thus far, the basic electrophysiological and synaptic properties of D2(+) and D2(-) MSNs in the NAc core are similar to those exhibited by MSNs in the dorsal striatum<sup>6, 16</sup>. Notably, robust LTD can be generated in D2(+) MSNs, but not D2(-) MSNs in both structures. It was therefore surprising to find that unlike LTD in dorsal striatal D2(+) MSNs, the LFS LTD in NAc core D2(+) MSNs was reduced but clearly not blocked by the CB1 receptor antagonist AM251 (1–5  $\mu$ M) (Fig. 3a:  $75 \pm 5\%$ ,  $n = 12$ ). This was not due to lack of efficacy of AM251 as its prior application (at 1  $\mu$ M) prevented the depression of EPSCs in D2(+) MSNs caused by the CB1 receptor agonist WIN 55,212 (Fig. 3b: WIN followed by AM251,  $58 \pm 9\%$  of baseline,  $n = 4$ ; AM251 followed by WIN,  $98 \pm 3\%$  of baseline,  $n=4$ ). Because the presynaptic active zone protein RIM1 $\alpha$  plays a critical role in several types of presynaptic plasticity including eCB-LTD at some synapses<sup>18</sup> we tested the role of RIM1 $\alpha$  in LFS LTD at D2(+) synapses by crossing the BAC transgenic D2-EGFP mice with *RIM1 $\alpha$ <sup>-/-</sup>* mice<sup>19</sup>. Similar to the effects of AM251, LFS LTD in NAc core D2(+) MSNs in the *RIM1 $\alpha$ <sup>-/-</sup>* mice was reduced, but not absent, compared to littermate controls (Fig. 3c: *RIM1 $\alpha$ <sup>-/-</sup>*,  $82 \pm 8\%$ ,  $n = 8$ ; littermates,  $40 \pm 6\%$   $n = 6$ ). DHPG-induced synaptic depression in D2(+) MSNs was also reduced, but not blocked, in the *RIM1 $\alpha$ <sup>-/-</sup>* mice (Fig. 3d: *RIM1 $\alpha$ <sup>-/-</sup>*,  $83 \pm 8\%$ ,  $n = 4$ ; littermates,  $54 \pm 7\%$ ,  $n = 4$ ). These results extend previous studies of eCB-LTD in the NAc<sup>17, 18, 20</sup> by demonstrating that it is restricted to D2(+) neurons in the NAc core and requires the active zone protein RIM1 $\alpha$ . However, these results also indicate that a CB1- and RIM1 $\alpha$ -independent form of LTD exists at these same synapses.

## TRPV1 activation plays a role in LFS-LTD in NAc D2(+) MSNs

Although the main target for endocannabinoid signaling at synapses is thought to be the CB1 receptor, the endocannabinoid anandamide can also activate TRPV1 (transient receptor potential vanilloid 1) channels<sup>10–13</sup>. TRPV1 is a nonselective cation channel that is highly permeable to calcium and is the main target for capsaicin, the pungent ingredient in chili peppers. Recent work has shown that activation of presynaptic TRPV1 channels is required for LTD triggered by postsynaptic mGluRs at excitatory synapses on interneurons in the hippocampus<sup>14</sup> and in the developing superior colliculus<sup>15</sup>. Furthermore, anatomical studies suggest that TRPV1 is present in many brain structures including the NAc<sup>11, 21–23</sup>. We therefore tested the possibility that the LFS LTD remaining in the *RIM1α*<sup>-/-</sup> mice and in the presence of AM251 involves TRPV1 channels by examining the effects of two structurally distinct TRPV1 competitive antagonists. Application of either capsazepine (10 μM) or SB366791 (20 μM) clearly reduced but did not block LFS LTD in D2(+) MSNs (Fig. 4a, b: 81 ± 5%, n = 6; 85 ± 3%, n = 6). Application of capsazepine alone had no effect on basal AMPAR EPSCs (data not shown; 101 ± 6%, n = 5) suggesting that there is no constitutive activity of TRPV1. When CB1 receptors and TRPV1 channels were both antagonized by simultaneous application of AM251 and capsazepine, LFS-LTD was absent (Fig. 4c: 97 ± 8%, n = 7). Furthermore, the LFS LTD remaining in D2(+) MSNs in the *RIM1α*<sup>-/-</sup> mice (see Fig. 3c) was blocked by the TRPV1 antagonist capsazepine (Fig. 4d: 99 ± 14%, n = 4).

The inhibitory effects of two different TRPV1 antagonists on LFS LTD in D2(+) MSNs suggests that TRPV1 channels are required for this form of synaptic plasticity. To test whether activation of TRPV1 channels alone can trigger LTD, we applied the specific TRPV1 agonist capsaicin while recording AMPAR EPSCs. Capsaicin (3 μM) caused a depression of AMPAR EPSCs in D2(+) neurons that did not reverse following its wash-out (Fig. 4e: 70 ± 5%, n = 19). Following capsaicin application and wash-out, LFS-LTD in D2(+) MSNs was reduced (Fig. 4f: 74 ± 12%, n = 4), a result consistent with a partial occlusion of LFS LTD. The effects of capsaicin on AMPAR EPSCs recorded from D2(+) neurons were prevented by prior application of the TRPV1 antagonist, capsazepine, (Fig. 4g: 99 ± 9%, n = 5) but not prior application of the CB1 receptor antagonist, AM251 (Fig. 4h: 77 ± 10%, n = 7).

Although the results of the pharmacological manipulations which antagonize or activate TRPV1 channels are consistent with a key role for these channels in LFS LTD, the interpretation of the results are dependent on the specificity of the drugs we used. Therefore, to further test the role of TRPV1 in modulating synaptic transmission in D2(+) cells in the NAc core, we crossed the D2-EGFP BAC transgenic mice with *TRPV1*<sup>-/-</sup> mice (Jackson Labs). LFS LTD in D2(+) MSNs in the *TRPV1*<sup>-/-</sup> mice was reduced compared to littermate controls (Fig. 5a: *TRPV1*<sup>-/-</sup>, 82 ± 8%, n = 9; wildtype, 56 ± 4%, n = 5) and this remaining LTD was blocked by AM251 (Fig. 5b: 107 ± 7%, n = 5). Furthermore, capsaicin no longer depressed AMPAR EPSCs in the *TRPV1*<sup>-/-</sup> mice while causing a depression in wildtype controls (Fig. 5c: *TRPV1*<sup>-/-</sup>: 105 ± 8%, n = 6; wildtype 70 ± 5%, n = 14). The results of the pharmacological experiments and those from the *TRPV1*<sup>-/-</sup> mice provide support for the existence of a bifurcating signaling pathway in D2(+) MSNs. Specifically, we propose that activation of postsynaptic mGluR5 leads to the production of lipid signaling molecules that activate TRPV1 channels and CB1 receptors, each of which in turn triggers LTD at excitatory synapses on D2(+) MSNs in the NAc core.

## Postsynaptic locus of TRPV1 function in NAc D2(+) MSNs

In most brain structures, including the NAc, CB1 receptors are presynaptic and modify transmitter release<sup>18</sup>. However, the synaptic site of action of TRPV1 channels in the NAc is unknown. To address this issue we first determined whether the coefficient of variation

(CV) of the EPSCs changed during LFS LTD since changes in this measure are commonly associated with presynaptic forms of synaptic plasticity. In control conditions, LFS LTD caused a decrease in  $1/CV^2$  (Fig. 6a). This decrease is likely due to the CB1 receptor-mediated component of LFS LTD as no change in  $1/CV^2$  occurred when LTD was elicited during blockade of CB1 receptors by AM251 (Fig. 6a) while a decrease in  $1/CV^2$  still occurred when TRPV1 channels were blocked by antagonists (Fig. 6a). Consistent with this conclusion, the depression of AMPAR EPSCs elicited by the CB1 receptor agonist WIN caused a decrease in  $1/CV^2$  while the depression caused by capsaicin did not (Fig. 6b). As a second assay for the locus of action of TRPV1 channels in NAc D2(+) MSNs we examined the effects of capsaicin on miniature EPSCs (mEPSCs). Capsaicin application did not alter mEPSC frequency but did reduce mEPSC amplitudes (Fig. 6c; frequency, pre capsaicin,  $4.02 \pm 1.44$  Hz versus  $4.41 \pm 1.20$  Hz post capsaicin; amplitude, pre capsaicin  $22.98 \pm 2.17$  pA versus  $18.16 \pm 1.04$  pA post capsaicin,  $n = 6$ ). We also examined the effects of capsaicin on NMDA receptor-mediated EPSCs (NMDAR EPSCs) since manipulations that presynaptically depress transmitter release commonly depress both AMPAR- and NMDAR EPSCs to equal extents. Capsaicin had no effect on pharmacologically isolated NMDAR EPSCs recorded at either  $-50$  mV or  $+40$  mV (Fig 6d:  $110 \pm 7\%$ ,  $n = 4$  and  $101 \pm 7\%$ ,  $n = 6$ , respectively).

Taken together, these results suggest that the TRPV1 channels involved in LFS LTD are localized to postsynaptic D2(+) MSNs in the NAc. Indeed, postsynaptic TRPV1 has been found to be colocalized with presynaptic CB1 receptors in the NAc core<sup>21</sup>. Consistent with the postsynaptic expression of TRPV1 channels, loading D2(+) MSNs with capsazepine ( $2 \mu\text{M}$ ) or SB366791 ( $4 \mu\text{M}$ ), significantly attenuated LFS-LTD relative to vehicle controls (Fig. 6e; TRPV1 antagonists,  $88 \pm 6\%$ ,  $n = 8$ ; vehicle control,  $56 \pm 8\%$ ,  $n = 7$ ). As TRPV1 activation causes a rise in intracellular  $\text{Ca}^{2+}$  concentration<sup>10–12</sup>, which is a common trigger for synaptic plasticity, we next loaded D2(+) cells with the  $\text{Ca}^{2+}$  chelator EGTA and found that this manipulation prevented the synaptic effects of capsaicin (Fig. 6f:  $99 \pm 1\%$ ,  $n = 8$ ). Purely postsynaptic forms of LTD often are due to the  $\text{Ca}^{2+}$ -triggered endocytosis of AMPARs<sup>3</sup>. To test whether this expression mechanism underlies the TRPV1-triggered LTD in the NAc, we loaded D2(+) MSNs with either a dynamin inhibitory peptide (D15)<sup>24</sup>, or a scrambled version of the peptide (S15). This manipulation prevented LFS LTD induced in the presence of AM251 (Fig. 6g:  $104 \pm 9\%$ ,  $n=4$  vs.  $66 \pm 9\%$ ,  $n=3$ ).

A plausible model that explains all of our results is that postsynaptic mGluR activation in NAc D2(+) MSNs leads to the production of anandamide, an endocannabinoid that activates both CB1 receptors and TRPV1 channels<sup>10–13, 18, 23</sup>. To test this hypothesis, we isolated the TRPV1-triggered LTD by application of AM251 and inhibited the anandamide degrading enzyme fatty acid amide hydrolase (FAAH) by applying URB597 ( $1 \mu\text{M}$ ). LFS LTD in slices preincubated in URB597 plus AM251 was enhanced relative to AM251 alone (Fig. 6h:  $48 \pm 8\%$ ,  $n=6$ ;  $75 \pm 5\%$ ,  $n=12$ ), a result consistent with a key role of anandamide. To test whether anandamide is also capable of enhancing eCB-LTD, we examined the effects of URB597 on the LTD elicited in D2(+) MSNs in slices prepared from the *TRPV1*<sup>-/-</sup> mice. This manipulation enhanced LFS LTD (Fig. 6i:  $52 \pm 11\%$ ,  $n=7$ ) suggesting that anandamide does activate both presynaptic CB1 receptors and postsynaptic TRPV1 channels in NAc D2(+) MSNs in the presence of the FAAH inhibitor. This finding offers a starting point for future work to determine whether anandamide or another lipid signaling molecule is responsible for activating CB1 receptors and TRPV1 channels under basal conditions.

### Effect of cocaine on LTD and sensitization in *TRPV1*<sup>-/-</sup> mice

*In vivo* administration of drugs of abuse impairs eCB-LTD in the NAc<sup>20, 25, 26</sup>. Consistent with these prior results, LFS LTD in D2(+) MSNs in the NAc core 24 hours following administration of a single dose of cocaine was absent whereas *in vivo* saline injections had

no effect on LTD (Fig. 7a; cocaine,  $93 \pm 6\%$ ,  $n = 6$ ; saline,  $62 \pm 3\%$ ,  $n = 5$ ). To test specifically whether the synaptic depression caused by direct TRPV1 activation is affected by prior *in vivo* cocaine exposure, we bath applied capsaicin to slices prepared from cocaine and saline treated animals. The synaptic depression elicited by capsaicin was unaffected by prior cocaine treatment (Fig. 7b; cocaine,  $78 \pm 7\%$ ,  $n = 7$ ; saline,  $83 \pm 3\%$ ,  $n = 9$ ). These results are consistent with the suggestion that *in vivo* administration of cocaine impairs postsynaptic mGluR signaling, which is required for initiation of downstream eCB production in NAc MSNs<sup>25</sup>, thus resulting in the absence of both CB1- and TRPV1-dependent LTD.

A critical question for any form of synaptic plasticity is whether it plays a behaviorally meaningful role in the context of the brain region in which it is observed<sup>27</sup>. As an initial test of whether TRPV1 function in the NAc plays a role in the behavioral responses to cocaine, we examined behavioral sensitization to cocaine in the *TRPV1*<sup>-/-</sup> mice. Behavioral sensitization is a robust form of drug-induced behavioral plasticity that involves long-lasting modifications in NAc circuitry and correlates well with the enhanced incentive properties of drugs of abuse due to repetitive exposure<sup>28</sup>. While basal locomotor activity following saline injections was normal in the *TRPV1*<sup>-/-</sup> mice, cocaine-induced locomotor activity was enhanced in *TRPV1*<sup>-/-</sup> mice relative to wildtype controls (Fig. 7c). This enhancement was maintained as behavioral sensitization developed following repeated daily administration of cocaine (Fig. 7c). Furthermore, the enhanced locomotor response to cocaine in the *TRPV1*<sup>-/-</sup> mice was maintained 2 weeks after cessation of the 5 days of repetitive cocaine administration (Fig. 7c). In contrast, cocaine-induced stereotypy, which is thought to be due to activation of dorsal striatal circuits, was normal in the *TRPV1*<sup>-/-</sup> mice (Fig. 7d).

## DISCUSSION

We have presented an extensive electrophysiological characterization of indirect and direct pathway MSNs in the NAc core and found that several properties are similar to those previously described for MSNs in dorsal striatum<sup>6, 16</sup>. Indirect pathway MSNs are more excitable and their excitatory synapses have a higher probability of release. Importantly, LTD induced by LFS is limited to indirect pathway D2(+) MSNs and is, in part, CB1 receptor-dependent. However, in addition, we demonstrate the existence of a novel form of LTD that requires activation of postsynaptic TRPV1 channels and is likely due to endocytosis of AMPARs. Our results suggest that strong postsynaptic mGluR5 activation in D2(+) NAc MSNs produces one or more endocannabinoid(s) that simultaneously activate(s) presynaptic CB1 receptors and postsynaptic TRPV1 channels (Supplemental Fig. 1). They also suggest that activation of the postsynaptic TRPV1 channels in turn leads to a rise in postsynaptic calcium that like other extensively studied forms of postsynaptic LTD causes endocytosis of AMPARs<sup>3, 27</sup>.

Although the activation of presynaptic CB1 receptors and postsynaptic TRPV1 channels could be achieved by the generation of two different endocannabinoids in D2(+) NAc MSNs, the enhancement of both TRPV1- and CB1-mediated LTD by the FAAH inhibitor URB597 suggests that anandamide may trigger both forms of plasticity. Consistent with this hypothesis, anandamide is generated by coupling of metabotropic receptors to Gq/11 family G proteins<sup>29</sup> and has been shown to activate TRPV1 channels in sensory neurons<sup>30</sup>. Furthermore, in the dorsal striatum, activation of TRPV1 by anandamide reduces levels of 2-arachidonoylglycerol (2-AG)<sup>31</sup>, an effect that would hinder the generation of eCB-LTD if 2-AG was the endocannabinoid produced by D2(+) NAc MSNs. In independent studies, a similar, if not identical, form of postsynaptic TRPV1-triggered LTD has been identified at a subpopulation of synapses on dentate gyrus granule cells<sup>32</sup>. Thus, this novel postsynaptic TRPV1-dependent form of synaptic plasticity is expressed in distinct cell types (i.e.

inhibitory NAc MSNs and excitatory granule cells) and is pathway specific in different brain regions (i.e. NAc and hippocampus) suggesting it may be a promiscuous form of plasticity that is important for modulating specific neural circuit elements throughout the brain.

TRPV1 channels are most prominently expressed in the peripheral nervous system but anatomical, behavioral, and electrophysiological studies have provided evidence for a role of TRPV1 channels in central nervous system function<sup>11, 14, 15, 23, 33</sup>. This has made TRPV1 a potentially attractive therapeutic target for indications beyond pain syndromes<sup>11, 23</sup>. In the context of the functional role of TRPV1 channels in striatal circuitry, a number of studies have reported pharmacological activation or inhibition of TRPV1 channels influences locomotor behavior in wildtype mice as well as hyperdopaminergic mice lacking the DA transporter<sup>34–37</sup>. Consistent with previous results<sup>33</sup>, we found that *TRPV1*<sup>-/-</sup> mice exhibit normal basal locomotor activity. However, they expressed enhanced, long-lasting locomotor sensitization to repetitive administration of cocaine, a form of behavioral plasticity that requires modification of NAc circuitry<sup>2, 3, 28</sup>. We also found that cocaine administration *in vivo* prevented the generation of both eCB-LTD and TRPV1-dependent LTD, an effect that can be explained by the attenuation of mGluR5 signaling caused by cocaine<sup>2, 25, 38</sup>. Alternatively *in vivo* cocaine exposure may impair endocannabinoid/endovanilloid synthesis and/or release independent of effects on mGluR5. It is also possible that CB1 receptor and TRPV1 function are reduced following cocaine exposure although this is unlikely because capsaicin-induced (Fig. 7b) and WIN-induced depression of synaptic transmission were normal in cocaine treated mice<sup>25</sup>. These observations on the effects of cocaine are all consistent with the hypothesis that TRPV1 channels in the NAc have a behaviorally important role although additional experiments clearly are required to determine whether TRPV1 channels specifically within the NAc influence cocaine-induced behaviors.

Previous work has suggested that drugs of abuse elicit LTD within the NAc and this is associated with the expression, not inhibition, of behavioral sensitization<sup>39–41</sup>. However, this form of LTD is NMDAR-dependent and since it is expressed in both indirect and direct pathway NAc MSNs, its triggering would be expected to have a very different behavioral role than pathway specific modifications. Indeed, modulation of activity specifically within the NAc indirect pathway has been implicated in several addiction related behaviors including reinstatement of drug seeking<sup>42–44</sup> and conditioned place preference<sup>45</sup>. Furthermore, independent molecular manipulations of indirect pathway versus indirect pathway MSNs *in vivo* have directly demonstrated that these two cell types participate in very different behaviors<sup>7, 8</sup>. Given the critical importance of excitatory circuitry within the NAc for the development and maintenance of addiction and the growing evidence that indirect- and direct pathway MSNs participate in behaviorally independent circuits, the identification of a functional role for TRPV1 channels in NAc D2(+) MSNs provides a new target for furthering our understanding of the pathophysiology and treatment of addiction as well as other disorders involving NAc circuitry.

## METHODS

### Electrophysiology

Parasagittal slices (250  $\mu$ m) containing the NAc core were prepared from D2-EGFP heterozygotic BAC transgenic mice on a C57Bl/6j background (postnatal days 28–56) as described previously<sup>46</sup>. Briefly, following euthanasia under isoflurane brains were quickly removed and placed in an ice-cold low sodium/high sucrose dissecting solution. Slices were cut by adhering the two sagittal hemispheres of brain containing the NAc core to the stage of a Leica vibroslicer. Slices were allowed to recover for a minimum of 60 minutes in a submerged holding chamber (~25°C) containing artificial cerebrospinal fluid (ACSF) consisting of (in mM): 124 NaCl, 4.4 KCl, 2.5 CaCl<sub>2</sub>, 1.3 MgSO<sub>4</sub>, 1 NaH<sub>2</sub>PO<sub>4</sub>, 11 glucose,

and 26 NaHCO<sub>3</sub>. Slices were then removed from the holding chamber and placed in the recording chamber where they were continuously perfused with oxygenated (95% O<sub>2</sub>/5% CO<sub>2</sub>) ACSF at a rate of 2 mL/minute at 30±2°C. Picrotoxin (50 μM) was added to the ACSF to block GABA<sub>A</sub>-receptor mediated inhibitory synaptic currents.

Whole-cell voltage- and current-clamp recordings from MSNs were obtained using IR-DIC video microscopy. The NAc core was identified by the presence of the anterior commissure. D2-EGFP positive MSNs in the NAc core were identified by the presence of the anterior commissure and the presence of EGFP that was excited with UV light using a bandpass filter (HQ470/40×). MSNs lacking any detectable EGFP signal were defined as D2(-), rather than D1(+), because the absence of detectable fluorescence in a MSN in this mouse line does not unequivocally identify that the cell is a direct pathway MSN expressing D1 DA receptors. Recordings were made with electrodes (3.0–6.0 MΩ) filled with either (in mM): 120 CsMeSO<sub>4</sub>, 15 CsCl, 8 NaCl, 10 HEPES, 0.2 EGTA, 10 TEA-Cl, 4 Mg<sup>2+</sup>ATP, 0.3 Na<sup>2+</sup>GTP, 0.1 spermine and 5 QX-314 (for voltage clamp recordings) or 130 KMeSO<sub>3</sub>, 10 NaCl, 2 MgCl<sub>2</sub>, 0.16 CaCl<sub>2</sub>, 10 HEPES, 0.5 EGTA (for current clamp recordings). Excitatory afferents were stimulated with a bipolar nichrome wire electrode placed at the border between the NAc core and cortex dorsal to the anterior commissure. Recordings were performed using an Axopatch 1D or Multiclamp 700B (Molecular Devices), filtered at 2 kHz and digitized at 10 kHz. Excitatory postsynaptic currents (EPSCs) of 100–400 pA were evoked at a frequency of 0.1 Hz while MSNs were voltage-clamped at -70 mV unless otherwise stated. Data acquisition and analysis were performed online using custom Igor Pro software. Input resistance and access resistance were monitored continuously throughout the duration of each experiment, which were terminated if these changed by >20%. For experiments that involved postsynaptic loading of cells with compounds via the patch pipette solution, whole cell access was established and cells were held for 30 minutes prior to the initiation of the experiment.

Paired-pulse ratios (PPR) were acquired by applying a second afferent stimulus of equal intensity at a specified time after the first stimulus and then calculating EPSC1/EPSC2. For a given interstimulus interval for each cell, the PPR of 6 consecutive responses were averaged. NMDAR/AMPA ratios were calculated as the ratio of the magnitude of the EPSC recorded at +40 mV at 50 ms following afferent stimulation (NMDAR EPSCs) to the peak amplitude of the EPSC at -80 mV (AMPA EPSCs). Miniature EPSCs were collected at a holding potential of -70 mV in the presence of 500 nM TTX. Ten second blocks of events were acquired and analyzed using Mini-analysis software (Synaptosoft, Decatur, Georgia) with threshold parameters set at 5 pA amplitude and less than 3 ms rise time. All events included in the final data analysis were verified by eye. For current-clamp experiments, firing frequency was analyzed as the number of spikes occurring during a fixed current injection (800 ms).

Summary LTD graphs were generated by averaging the peak amplitudes of individual EPSCs in 1 minute bins (i.e. 6 consecutive sweeps) and normalizing these to the mean value of EPSCs collected during the 10 minute baseline immediately preceding the LFS. Individual experiments were then averaged together. The magnitude of LTD was calculated by averaging EPSC amplitudes during the last 10 minutes of the experiment (routinely at 25–35 or 35–45 minutes following the induction protocol) and comparing these to the average EPSC during the 10 minute baseline. We define LTD as a depression of EPSC amplitudes greater than 10% (i.e. EPSC amplitudes during the last 10 minutes of the experiment being less than 90% of the baseline EPSC amplitudes). For all experiments examining LTD or the application of capsaicin, recordings from control cells were interleaved with recordings from cells undergoing the experimental manipulation with a ratio of 1 control cell for every 2 to 4 experimental cells. Comparisons between different

experimental manipulations were made using a two-tailed Student's t-test with  $p < 0.05$  considered significant. All statements in the text regarding differences between grouped data indicate statistical significance was achieved. All values are reported as mean  $\pm$  s.e.m.

### ***In vivo* manipulations and assays**

Mice were housed in cages of 2 to 5 on a 12 hour light/dark cycle with food and water *ad libitum*. Four to five week old mice were given intraperitoneal (ip) injections of equal volumes of either cocaine (15 mg/kg) or saline in a novel environment and were returned to their home cages 15 minutes later. Mice were sacrificed and recordings were made 24 hours after the injection. Locomotor activity in the open-field test was measured using the ENV-510 test environment and Activity Monitor software (Med Associates Inc.). Mice received an ip injection and were immediately placed inside an 11  $\times$  11 inch box with three 16-beam IR arrays. Distance traveled (cm) and stereotypic behaviors were calculated over 15 minute blocks of time. Stereotypic behaviors were defined as time spent breaking beams within a restricted space around the mouse. For all experiments involving *in vivo* manipulations, data acquisition and analysis were performed blinded to the *in vivo* treatment. All animal procedures were in accordance with institutional guidelines (IACUC approved).

### **Data analysis**

Values are expressed as mean  $\pm$  s.e.m ( $n$  = number of cells). Two-tailed Student's test was used for statistical analysis and  $P$  values less than 0.05 were considered to be statistically significant.

### **Drugs**

The following drugs were purchased from Sigma-Aldrich (St. Louis, MO): cocaine HCl, picrotoxin, tetrodotoxin (TTX). The following reagents were purchased from Tocris (Ellisville, MO): D-APV, SCH23390, Sulpiride, LY341495, RS-DHPG, MPEP, LY367385, WIN55,212-2, AM251, Capsazepine, SB366791, Capsaicin, S15, D15. URB597 was purchased from Biomol International (now Enzo Life Sciences, Plymouth Meeting, PA).

### **Supplementary Material**

Refer to Web version on PubMed Central for supplementary material.

### **Acknowledgments**

We thank members of the Malenka lab for their helpful comments throughout the course of this project. This work was supported by grants from the National Institute on Drug Abuse (DA009264, DA008227 to RCM; 5F32DA023741-2 to BAG).

### **References**

1. Sesack SR, Grace AA. Cortico-Basal Ganglia reward network: microcircuitry. *Neuropsychopharmacol.* 2010; 35:27–47.
2. Kalivas PW. The glutamate homeostasis hypothesis of addiction. *Nat. Rev. Neurosci.* 2009; 10:561–572. [PubMed: 19571793]
3. Kauer JA, Malenka RC. Synaptic plasticity and addiction. *Nat. Rev. Neurosci.* 2007; 8:844–858. [PubMed: 17948030]
4. Conrad KL, et al. Formation of accumbens GluR2-lacking AMPA receptors mediates incubation of cocaine craving. *Nature.* 2008; 454:118–121. [PubMed: 18500330]
5. Kasanetz F, et al. Transition to addiction is associated with a persistent impairment in synaptic plasticity. *Science.* 2010; 328:1709–1712. [PubMed: 20576893]

6. Kreitzer AC, Malenka RC. Striatal plasticity and basal ganglia circuit function. *Neuron*. 2008; 60:543–554. [PubMed: 19038213]
7. Hikida T, Kimura K, Wada N, Funabiki K, Nakanishi S. Distinct Roles of Synaptic Transmission in Direct and Indirect Striatal Pathways to Reward and Aversive Behavior. *Neuron*. 2010; 66:896–907. [PubMed: 20620875]
8. Kravitz AV, et al. Regulation of parkinsonian motor behaviours by optogenetic control of basal ganglia circuitry. *Nature*. 2010; 466:622–626. [PubMed: 20613723]
9. Gong S, et al. A gene expression atlas of the central nervous system based on bacterial artificial chromosomes. *Nature*. 2003; 425:917–925. [PubMed: 14586460]
10. Caterina MJ, Julius D. The vanilloid receptor: a molecular gateway to the pain pathway. *Annu. Rev. Neurosci.* 2001; 24:487–517. [PubMed: 11283319]
11. Kauer JA, Gibson HE. Hot flash: TRPV channels in the brain. *Tr. Neurosci.* 2009; 32:215–224.
12. Ramsey IS, Delling M, Clapham DE. An introduction to TRP channels. *Annu. Rev. Physiol.* 2006; 68:619–647. [PubMed: 16460286]
13. Zygmunt PM, et al. Vanilloid receptors on sensory nerves mediate the vasodilator action of anandamide. *Nature*. 1999; 400:452–457. [PubMed: 10440374]
14. Gibson HE, Edwards JG, Page RS, Van Hook MJ, Kauer JA. TRPV1 channels mediate long-term depression at synapses on hippocampal interneurons. *Neuron*. 2008; 57:746–759. [PubMed: 18341994]
15. Maione S, et al. TRPV1 channels control synaptic plasticity in the developing superior colliculus. *J. Physiol.* 2009; 587:2521–2535. [PubMed: 19406878]
16. Kreitzer AC, Malenka RC. Endocannabinoid-mediated rescue of striatal LTD and motor deficits in Parkinson's disease models. *Nature*. 2007; 445:643–647. [PubMed: 17287809]
17. Robbe D, Kopf M, Remaury A, Bockaert J, Manzoni OJ. Endogenous cannabinoids mediate long-term synaptic depression in the nucleus accumbens. *Proc. Natl. Acad. Sci. USA*. 2002; 99:8384–8388. [PubMed: 12060781]
18. Heifets BD, Castillo PE. Endocannabinoid signaling and long-term synaptic plasticity. *Annu. Rev. Physiol.* 2009; 71:283–306. [PubMed: 19575681]
19. Schoch S, et al. RIM1alpha forms a protein scaffold for regulating neurotransmitter release at the active zone. *Nature*. 2002; 415:321–326. [PubMed: 11797009]
20. Hoffman AF, Oz M, Caulder T, Lupica CR. Functional tolerance and blockade of long-term depression at synapses in the nucleus accumbens after chronic cannabinoid exposure. *J. Neurosci.* 2003; 23:4815–4820. [PubMed: 12832502]
21. Micale V, et al. Anxiolytic effects in mice of a dual blocker of fatty acid amide hydrolase and transient receptor potential vanilloid type-1 channels. *Neuropsychopharmacol.* 2009; 34:593–606.
22. Roberts JC, Davis JB, Benham CD. [<sup>3</sup>H]Resiniferatoxin autoradiography in the CNS of wild-type and TRPV1 null mice defines TRPV1 (VR-1) protein distribution. *Brain Res.* 2004; 995:176–183. [PubMed: 14672807]
23. Starowicz K, Cristino L, Di Marzo V. TRPV1 receptors in the central nervous system: potential for previously unforeseen therapeutic applications. *Curr. Pharm. Des.* 2008; 14:42–54. [PubMed: 18220817]
24. Lüscher C, et al. Role of AMPA receptor cycling in synaptic transmission and plasticity. *Neuron*. 1999; 24:649–658. [PubMed: 10595516]
25. Fourgeaud L, et al. A single in vivo exposure to cocaine abolishes endocannabinoid-mediated long-term depression in the nucleus accumbens. *J. Neurosci.* 2004; 24:6939–6945. [PubMed: 15295029]
26. Mato S, et al. A single in-vivo exposure to Delta 9THC blocks endocannabinoid-mediated synaptic plasticity. *Nat. Neurosci.* 2004; 7:585–586. [PubMed: 15146190]
27. Malenka RC, Bear MF. LTP and LTD: an embarrassment of riches. *Neuron*. 2004; 44:5–21. [PubMed: 15450156]
28. Vezina P, Leyton M. Conditioned cues and the expression of stimulant sensitization in animals and humans. *Neuropharmacol.* 2009; 56(Suppl 1):160–168.

29. Wettschureck N, et al. Forebrain-specific inactivation of Gq/G11 family G proteins results in age-dependent epilepsy and impaired endocannabinoid formation. *Mol. Cell Biol.* 2006; 26:5888–5894. [PubMed: 16847339]
30. van der Stelt M, et al. Anandamide acts as an intracellular messenger amplifying Ca<sup>2+</sup> influx via TRPV1 channels. *Embo J.* 2005; 24:3026–3037. [PubMed: 16107881]
31. Maccarrone M, et al. Anandamide inhibits metabolism and physiological actions of 2-arachidonoylglycerol in the striatum. *Nat. Neurosci.* 2008; 11:152–159. [PubMed: 18204441]
32. Chavez AE, Chiu CQ, Castillo PE. TRPV1 activation by endogenous anandamide triggers postsynaptic LTD in dentate gyrus. *Nat. Neurosci.* 2010
33. Marsch R, et al. Reduced anxiety, conditioned fear, and hippocampal long-term potentiation in transient receptor potential vanilloid type 1 receptor-deficient mice. *J. Neurosci.* 2007; 27:832–839. [PubMed: 17251423]
34. de Lago E, de Miguel R, Lastres-Becker I, Ramos JA, Fernandez-Ruiz J. Involvement of vanilloid-like receptors in the effects of anandamide on motor behavior and nigrostriatal dopaminergic activity: in vivo and in vitro evidence. *Brain Res.* 2004; 1007:152–159. [PubMed: 15064146]
35. Di Marzo V, et al. Hypolocomotor effects in rats of capsaicin and two long chain capsaicin homologues. *Eur. J. Pharmacol.* 2001; 420:123–131. [PubMed: 11408034]
36. Lee J, Di Marzo V, Brotchie JM. A role for vanilloid receptor 1 (TRPV1) and endocannabinoid signalling in the regulation of spontaneous and L-DOPA induced locomotion in normal and reserpine-treated rats. *Neuropharmacol.* 2006; 51:557–565.
37. Tzavara ET, et al. Endocannabinoids activate transient receptor potential vanilloid 1 receptors to reduce hyperdopaminergia-related hyperactivity: therapeutic implications. *Biol. Psychiatry.* 2006; 59:508–515. [PubMed: 16199010]
38. Szumlinski KK, Kalivas PW, Worley PF. Homer proteins: implications for neuropsychiatric disorders. *Curr. Opin. Neurobiol.* 2006; 16:251–257. [PubMed: 16704932]
39. Thomas MJ, Beurrier C, Bonci A, Malenka RC. Long-term depression in the nucleus accumbens: a neural correlate of behavioral sensitization to cocaine. *Nat. Neurosci.* 2001; 4:1217–1223. [PubMed: 11694884]
40. Kourrich S, Rothwell PE, Klug JR, Thomas MJ. Cocaine experience controls bidirectional synaptic plasticity in the nucleus accumbens. *J. Neurosci.* 2007; 27:7921–7928. [PubMed: 17652583]
41. Brebner K, et al. Nucleus accumbens long-term depression and the expression of behavioral sensitization. *Science.* 2005; 310:1340–1343. [PubMed: 16311338]
42. McFarland K, Kalivas PW. The circuitry mediating cocaine-induced reinstatement of drug-seeking behavior. *J. Neurosci.* 2001; 21:8655–8663. [PubMed: 11606653]
43. Tang XC, McFarland K, Cagle S, Kalivas PW. Cocaine-induced reinstatement requires endogenous stimulation of mu-opioid receptors in the ventral pallidum. *J. Neurosci.* 2005; 25:4512–4520. [PubMed: 15872098]
44. Torregrossa MM, Tang XC, Kalivas PW. The glutamatergic projection from the prefrontal cortex to the nucleus accumbens core is required for cocaine-induced decreases in ventral pallidal GABA. *Neurosci. Lett.* 2008; 438:142–145. [PubMed: 18455875]
45. Durieux PF, et al. D2R striatopallidal neurons inhibit both locomotor and drug reward processes. *Nat. Neurosci.* 2009; 12:393–395. [PubMed: 19270687]
46. Grueter BA, et al. Extracellular-signal regulated kinase 1-dependent metabotropic glutamate receptor 5-induced long-term depression in the bed nucleus of the stria terminalis is disrupted by cocaine administration. *J. Neurosci.* 2006; 26:3210–3219. [PubMed: 16554472]

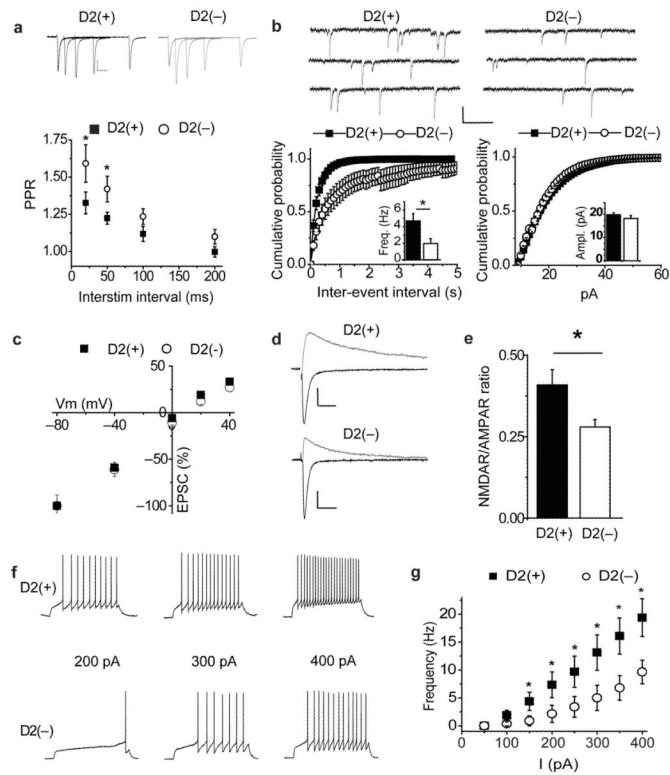


**Figure 1.**

Electrophysiological properties of direct [D2(+)] and indirect [D2(-)] pathway MSNs in the NAc core. **(a)** Sample traces of D2(+) and D2(-) EPSCs at 20, 50, 100 and 200 ms interstimulus intervals. Summary graph of paired-pulse ratios (PPR) from D2(+) (filled squares;  $n=18$ ) and D2(-) (open circles;  $n=11$ ) MSNs. (Calibration bars for evoked EPSCs in this panel and all subsequent figures unless noted are 50 pA / 25 ms.) **(b)** Sample traces of mEPSCs from D2(+) and D2(-) MSNs. (Calibration bars; 20 pA / 200 ms.) Cumulative probability plot of mEPSC frequencies (left) and amplitudes (right) recorded from D2(-) (open circles;  $n=9$ ) and D2(+) (filled squares;  $n=9$ ) MSNs. Insets show mean  $\pm$  s.e.m. for the two populations. **(c)** Summary of normalized EPSC amplitudes in D-APV (50  $\mu$ M) and with intracellular spermine (0.1 mM) as a function of membrane potential recorded from D2(-) (open circles;  $n=11$ ) and D2(+) (filled squares;  $n=10$ ) MSNs. **(d)** Representative traces of EPSCs recorded at -80 mV and +40 mV from a D2(+) MSN and D2(-) MSN. **(e)** Summary graph of the ratio of the NMDAR EPSC (measured at 50 ms after stimulus at +40 mV) over the peak AMPAR EPSC (peak current recorded at -80 mV) from D2(-) ( $n=11$ ) and D2(+) ( $n=10$ ) MSNs. **(f)** Representative current clamp traces recorded from D2(+) and D2(-) MSNs in response to 200, 300 and 400 pA, 800 ms current injections. (Calibration bars: 20 mV / 200 ms.) **(g)** Summary of firing frequency in D2(-) (open circles;  $n=11$ ) and D2(+) (filled squares;  $n=8$ ) MSNs in response to 800 ms current injections. (\* in this and all subsequent figures indicates  $p<0.05$ .)

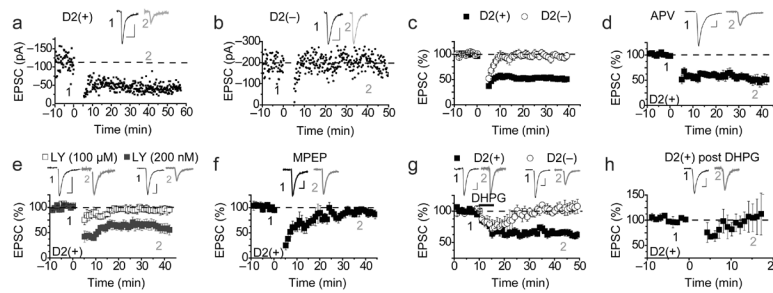


**Figure 2.**

D2(+) MSNs but not D2(-) NAc MSNs exhibit mGluR5-dependent LTD. **(a,b)** Timecourse of EPSC amplitude recorded from a representative D2(+) **(a)** and D2(-) **(b)** MSN before and after LFS (given at t=0). **(c)** Summary of EPSCs recorded from D2(+) (filled squares: n=25) and D2(-) (open circles: n=11) before and following LFS. **(d)** LFS LTD in D2(+) MSNs (n=6) is not blocked by D-APV (100 μM). **(e)** LTD in D2(+) MSNs is blocked by LY341495 at a concentration that blocks all mGluRs (open squares: 100 μM, n=6), whereas, a concentration specific for group II mGluRs (200 nM) has no effect (filled squares: n=6). **(f)** The mGluR5 negative allosteric modulator, MPEP (10 μM), blocks LTD at D2(+) synapses (n=5) **(g)** The group I mGluR agonist RS-DHPG (100 μM) induces LTD in D2(+) MSNs (filled squares: n=14) but not D2(-) MSNs (open circles: n=5). **(h)** LTD in D2(+) MSNs is occluded 40 min following DHPG application (n=4).

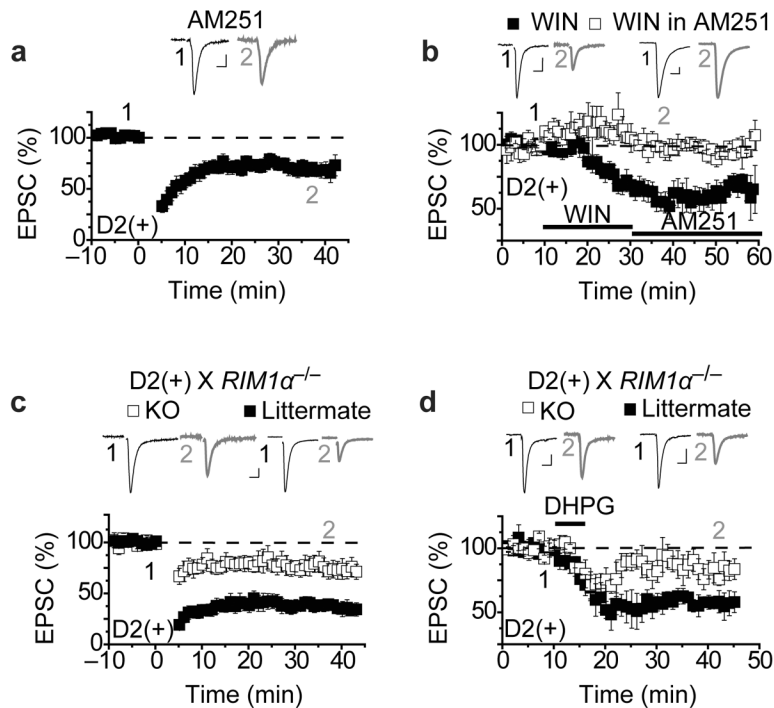


**Figure 3.**

D2(+) MSNs exhibit CB1 receptor/*RIM1α* dependent- and independent forms of LTD. **(a)** LTD in D2(+) MSNs is reduced but not blocked by the CB1 receptor antagonist AM251 (1–5 μM; n=12). **(b)** The CB1 receptor agonist WIN55,212-2 (1 μM) depresses synaptic transmission (filled squares: n=4), an effect that is blocked by prior application of AM251 (5 μM: open squares: n=4) but not by AM251 application following WIN application (filled squares). **(c)** LTD in D2(+) MSNs in *RIM1α*<sup>-/-</sup> mice (open squares: n=8) is reduced compared to LTD in littermate controls (filled squares: n=6). **(d)** DHPG-induced LTD in D2(+) MSNs is reduced in the *RIM1α*<sup>-/-</sup> mice (open circles: n=4) relative to littermate controls (filled squares: n=4).

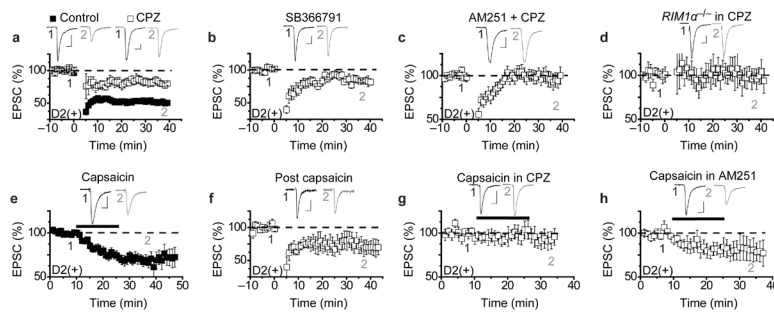


**Figure 4.**

TRPV1 channels trigger LTD at synapse on D2(+) NAc MSNs. **(a,b)** LFS LTD in D2(+) MSNs is reduced by the TRPV1 antagonists capsazepine (10  $\mu$ M) **(a)** (CPZ, open squares; n=6; controls, filled squares, n=25; graph from Fig. 2c) and SB366791 (20  $\mu$ M) **(b)**; n=6). **(c)** LTD in D2(+) MSNs is blocked by application of both AM251 and CPZ (n=7). **(d)** LTD in D2(+) MSNs in *RIM1 $\alpha$ <sup>-/-</sup>* mice is blocked by CPZ (n=5). **(e)** The TRPV1 agonist capsaicin (3  $\mu$ M) depresses AMPAR EPSCs in D2(+) MSNs (n=19). **(f)** LTD in D2(+) MSNs is reduced following capsaicin application (n=4). **(g)** Capsaicin-induced synaptic depression is blocked by the TRPV1 antagonist CPZ (n=5). **(h)** Capsaicin-induced synaptic depression is not blocked by AM251 (n=7).

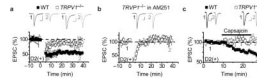


**Figure 5.** *TRPV1*<sup>-/-</sup> mice lack CB1 receptor-independent LFS LTD at synapses on D2(+) NAc MSNs. (a) LFS-LTD in D2(+) MSNs is reduced in *TRPV1*<sup>-/-</sup> mice (open squares, n=9) compared to wildtype littermates (filled squares, n=5). (b) The LTD remaining in D2(+) MSNs in *TRPV1*<sup>-/-</sup> mice is blocked by AM251 (n=5). (c) Capsaicin induces a depression of AMPAR EPSCs in D2(+) MSNs in wildtype mice (filled squares, n=14; these cells are a subset of those included in Fig. 4e and were selected because they were interleaved with the recordings from the *TRPV1*<sup>-/-</sup> slices) but not *TRPV1*<sup>-/-</sup> mice (open squares, n=6).

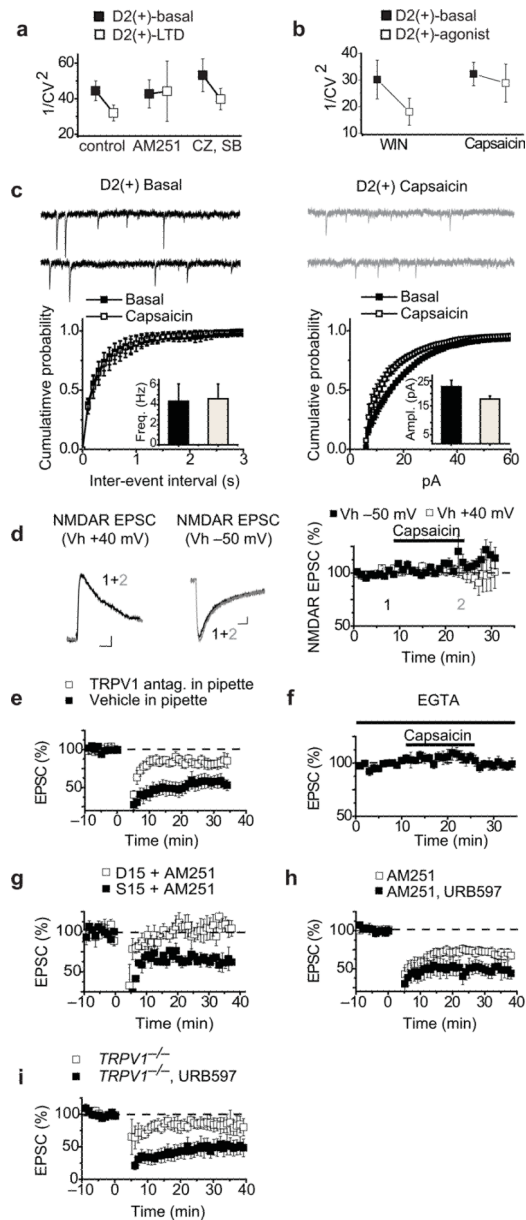


**Figure 6.**

Postsynaptic TRPV1 channels trigger LTD in D2(+) NAc MSNs. **(a)** Control LTD ( $n=25$ ) and eCB-LTD ( $n=23$ ) (pharmacologically isolated by TRPV1 antagonists) elicit a decrease in  $1/CV^2$  of AMPAR EPSCs whereas no change in  $1/CV^2$  is observed during TRPV1-dependent LTD ( $n=12$ ) (pharmacologically isolated by AM251). **(b)** Application of the CB1 agonist WIN reduces  $1/CV^2$  ( $n=4$ ) but application of the TRPV1 agonist capsaicin does not ( $n=14$ ). **(c)** Representative traces of mEPSCs before and after capsaicin application. Cumulative probability plots of capsaicin-induced changes in mEPSC frequencies (left,  $n=6$ ) and amplitudes (right). Insets show mean  $\pm$  s.e.m. **(d)** Representative traces of NMDAR EPSCs before and after capsaicin at +40 mV and -50 mV. (Calibration bars; 25 pA/25 ms.) Summary graph showing that application of capsaicin has no effect on NMDAR EPSCs at either holding potential ( $n=4$  at -50 mV and  $n=6$  at +40 mV). **(e)** Postsynaptic loading of the TRPV1 antagonist CPZ or SB366791 (open squares;  $n=12$ ) reduces LTD in D2(+) MSNs compared to vehicle loaded controls (filled squares;  $n=7$ ). **(f)** Postsynaptic loading of the

calcium chelator EGTA (20 mM) prevents capsaicin-induced depression of AMPAR EPSCs (n=8). **(g)** Postsynaptically loading the dynamin inhibitory peptide D15 but not the scrambled peptide S15 in the presence of AM251 prevents LTD in D2(+) MSNs (n=4, 3). **(h)** LTD is enhanced in slices incubated with the FAAH inhibitor URB597 (1  $\mu$ M) and AM251 (3  $\mu$ M) (filled squares; n=6) compared to AM251 alone (open squares, n=12). **(i)** LTD is enhanced in slices from *TRPV1*<sup>-/-</sup> mice incubated with the FAAH inhibitor URB597 (1  $\mu$ M; filled squares; n=6) compared to *TRPV1*<sup>-/-</sup> (open squares, n=9; these cells are the same as represented in Fig. 5a).

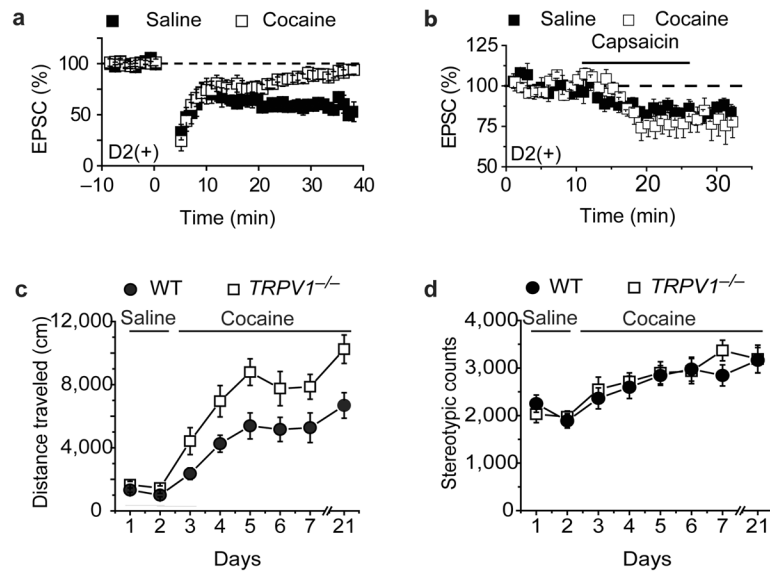


**Figure 7.**

Effects of *in vivo* cocaine administration on LFS LTD in NAc D2(+) MSNs and locomotor behavior in *TRPV1*<sup>-/-</sup> mice. **(a)** LFS LTD in D2(+) MSNs is absent 24 hours following administration of a single dose of cocaine (open squares, n=6) whereas it is normal following single saline injections (filled squares, n=5). **(b)** The depression of AMPAR EPSCs elicited by capsaicin is not affected by prior administration of a single dose of cocaine (open squares, n=7) or saline (filled squares, n=9). **(c)** *TRPV1*<sup>-/-</sup> mice (n=10; open squares) exhibit enhanced cocaine-induced locomotor activity relative to wildtype mice (n=12; filled circles). **(d)** Timecourse of cocaine-induced changes in stereotypic behaviors in *TRPV1*<sup>-/-</sup> and wildtype mice.